COMMUNICATION

Check for updates

Synthesis of fluorescent carbon nanoparticles by dispersion polymerization of acetylene†

Vijay Kumar Jayswal, [iD] Anna M. Ritcey [iD] and Jean-François Morin [iD]*

Carbon nanoparticles (CNPs) are of interest due to their distinct optoelectronic properties for a diverse range of applications and their functions and properties can be changed by varying their shape, size and dimensionality. The current synthetic methods reported often result in uncontrolled shape, size and polydispersity. In this work, we focus on developing a low-temperature synthetic method for preparing fluorescent carbon nanoparticles and modulation of properties. Our method, based on the dispersion Glaser–Hay polymerization of acetylene followed by decomposition into a carbonaceous material, yields CNPs with sizes varying from 30 nm to 60 nm. The change in reaction parameters influences the shape and size of CNPs, yielding spherical CNPs. The residual alkynes were exploited further for post-functionalization/graphitization by UV irradiation to yield multifunctional CNPs, which were fluorescent in the blue region. The CNPs were characterized with microscopy and spectroscopy techniques after synthesis and after UV-irradiation to study the morphological, chemical, physical and optical properties. This allowed us to understand the influence of parameter variation on the properties and to attempt to establish the structure–property relationship.

Introduction

Carbon nanoparticles (CNPs) have emerged as promising materials due to their unique photoluminescence properties[1,2] photostability[3] and low toxicity,[4] making them highly sought after for various applications.[5,6] Depending on the morphology, these properties can be varied by changing the size and shape of the CNPs.[7,8] Despite their numerous advantages, their implementation from laboratory to industrial products has been slowed due to their challenging synthesis, purification and the difficulty of controlling their size. Also, most of the synthetic

Département de Chimie et Centre de Recherche des Matériaux Avancés (CERMA), Université Laval, 1045, de la Médecine, Québec, Quebec, G1V 0A6, Canada. E-mail: jean-fancois.morin@chm.ulaval.ca

methods reported until now involve high-temperature (>100 °C) processes, which often result in uncontrolled shape and size and, consequently, uncontrolled properties. Moreover, the CNPs thus obtained are chemically inert, increasing the difficulty to modulate their properties using post-synthesis methods.

One method that has been explored for the synthesis of carbon nanomaterials under mild conditions is the use of metastable, sp-carbon-rich molecules as a precursor.[9–11] When assembled, these molecules can decompose into carbon nanomaterials of various shapes and sizes.[12,13] However, this method does not provide full control over the properties or the shape/size of nanoparticles for wider applications.[14,15] Several research groups made progress lately in synthesizing CNPs with this method. Hence, spherical,[16] tubular[17] and lamellar[18] CNPs have been prepared through the self-assembly of sp-carbon rich precursors, but in most cases, polydisperse nanoparticles have been obtained. Moreover, the long and tedious synthesis and self-assembly of the sp-carbon-rich precursors limit the use of these methods for the production of a large quantity of CNPs.

Recently, our group has made progress towards the use of a simple alkyne source for the preparation of CNPs with controlled morphology. In two straightforward steps, we prepared 1,4-bis(trimethylsilyl)-1,3-butadiyne and 1,2-bis(-trimethylsilylbutadiynyl)benzene, which were polymerized using metal-catalyzed polycondensation dispersion polymerization to form metastable polyyne intermediates that further decompose into CNPs.[19] This method offers an interesting means to exploit the high reactivity of alkynes under mild conditions, clearing the path to the use of a simple sp-carbon-rich source to synthesize CNPs at low temperatures.

An attractive alternative to complex alkyne-containing precursors would be to use gaseous acetylene as the sp-carbon-rich precursor. Acetylene has been used as a carbon source for synthesizing carbon nanomaterials at high temperatures using chemical vapor deposition (CVD),[20,21] laser-irradiation,[22] flame method,[23] catalytic/thermal decomposition techniques[24–26] plasma,[27] or various other methods[28–31] but it has

only been scarcely used as a carbon source for the preparation of carbon nanomaterials in solution at low temperature.[32] Although several reports on the preparation of polyynes (or carbynes) from acetylene polymerization have been published in the past decades, attempts to control the morphology of resulting materials, which is often the result of their decomposition into carbonaceous materials, are scarce. The difficulty of controlling the morphology comes from the high reactivity of polyynes, which are prone to addition reactions to give a random network of sp and sp^2 carbon atoms.[33–36]

Herein, we push the concept even further by synthesizing CNPs directly from acetylene gas using a low-temperature Glaser-type dispersion polymerization, allowing the synthesis of spherical and tubular CNPs with relatively narrow size distributions. The synthesis was conducted by bubbling acetylene gas directly in the reaction medium in ambient conditions. Acetylene underwent Pd catalyzed oxidative coupling in a dispersion polymerization medium. We assume that under these conditions, alkynes reacted quickly to form unstable, long polyynes that eventually decompose through a series of additions/cyclization processes within a confined environment (nanosize spheres) to form a disordered carbon-rich material.[13,37] The synthesized CNPs were irradiated with UV-light as a post-polymerization treatment to promote further polymerization of residual alkynes and functionalization/graphitization to yield multifunctional CNPs with new optical properties.

Results and discussion

The first report of the synthesis of conjugated polymer-based nanoparticles using Suzuki–Miyaura dispersion polymerization was published in 2012 by Kuehne and coworkers.[38–41] More recently, our group adapted this protocol to perform Glaser-type Pd/Cu-catalyzed dispersion polymerization for the preparation of carbon nanoparticles using 1,2-bis((trimethylsilyl)butadiynyl)benzene and 1,4-bis(trimethylsilyl)-1,3-butadiyne.[19,42] In the present study, we employ the same conditions with acetylene as the monomer as shown in Scheme 1.[43]

First, reactions at different temperatures and time duration were performed to study their influence on the resulting CNPs and the results are summarized in Table 1. The first set of reactions has been run for four hours as per the conditions optimized previously.[19,42] Then, for the second set of reactions, the mixture was stirred for 16 hours while continuously supplying acetylene to the reaction mixture, allowing polymerization to continue during the entire time of the reaction. The CNPs were purified by centrifugation and exchange of supernatant (see the ESI section for the details†).

Scheme 1 Synthesis of carbon nanoparticles using the Glaser-type Pd/Cu-catalyzed dispersion polymerization of acetylene.

Table 1 Details of reactions and experimental conditions with resulting nanoparticles size as determined from TEM images

Entry	Temperature (°C)	Time (h)	Size (nm)
1	25	4	53 ± 6
2	50	4	46 ± 12
3	70	4	44 ± 9
4	25	16	42 ± 9
5	50	16	47 ± 8
6	70	16	43 ± 9

When the reaction was performed at 25 °C for 4 hours (entry 1, Table 1), CNPs with an average size of 53 ± 6 nm (Fig. S1†) were formed. Increasing the reaction temperature (entries 2 and 3, Table 1) resulted in similar CNPs sizes (46 ± 12 nm and 44 ± 9 nm at 50 °C and 70 °C, respectively) accompanied by the formation of large aggregates of CNPs (Fig. S2 and S3†). Moreover, a relative decrease in the polydispersity index as measured by dynamic light scattering (DLS) (Fig. S8–S10 and Table S1†) was also observed when the reaction temperature was increased. The narrower size distribution and decrease in polydispersity might be attributed to a better solubility of the polyyne intermediate as the temperature is increased, retarding precipitation in the reaction medium. However, the formation of aggregates when the reaction was performed at a higher temperature is not fully understood.

To assess the influence of time on the CNPs morphology, a new set of reactions for which the reaction time remained unchanged at 16 hours was conducted (entries 4–6, Table 1). It was hypothesized that the longer reaction time would increase the decomposition of polyynes. The reaction performed at 25 °C (entry 4) resulted in CNPs aggregation (Fig. S4†) with the average size of the nanoparticle at 42 ± 9 nm. The longer reaction time might have increased the decomposition of polyynes resulting in the formation of more nanoparticles and an increase in temperature will increase the reaction rate. This will lead to more particles being formed and a higher concentration of nanoparticles present in the reaction. The aggregation observed may therefore be the result of a higher concentration of nanoparticles. The reaction at 50 °C for 16 hours also resulted in aggregation of CNPs with almost similar size (Fig. S5†) to that of the 4 hour reaction but also shows few tubular structures (Fig. S6†) being formed alongside spherical CNPs. The presence of tubular CNPs in the aggregation was also observed in an earlier reaction (Fig. S1c†). It can be hypothesized that the formation of tubular CNPs might be attributed to the change in the concentration of the reaction mixture during the course of the reaction as the continuous acetylene bubbling causes the evaporation of a small amount of solvent. The CNPs synthesized at 70 °C for 16 hours show uniform distribution of CNPs with size averaging 43 ± 9 nm (Fig. 1 and S7†) and negligible aggregation. The polydispersity index is changing with an increase in the temperature for this set of reactions too (Fig. S11–S13 and Table S1†). As observed in Table S1,† the

Fig. 1 (a) TEM image and (b) size histogram of CNPs synthesized at 70 °C for 16 hours.

increased reaction time and temperature seem to impact the polydispersity index.

To observe the batch-to-batch consistency of resulting CNPs, repetition experiments were performed under on the same reaction conditions and the resulting CNPs follow similar patterns to the previous reactions as shown in the TEM images and size histogram data (Fig. S1e, S2e, S4e and S7d–f†). The scale-up reaction at a scale of 10 times was performed for the CNPs synthesized at 70 °C for 16 hours and the resulting CNPs (Fig. S7g†) show similar size and distribution pattern as the standard scale reactions.

It can be concluded that the size of CNPs could be influenced by the variation in reaction temperature and time. The variation in reaction parameters leads to achieving the synthesis of spherical CNPs with uniform size distribution. Utilizing acetylene gas as a source in low-temperature polymerization methods would provide a sustainable route for low-cost synthesis of carbon nanomaterials. Though, utilizing acetylene gas by bubbling in the reaction mixture causes the evaporation of the solvent, changing the concentration of the reaction mixture and resulting in random changes in CNPs shapes. If a controlled environment can be created to run the reaction

with a pressure reactor for utilizing the acetylene, it would reduce solvent evaporation or change in the concentration of the reaction mixture and provide better control over the shape and size of CNPs. It would also provide an opportunity to utilize the pressure of acetylene gas as a reaction parameter.

The CNPs were further characterized to study their properties and chemical composition. The selected area electron diffraction (SAED) patterns (Fig. S14 and S15†) were recorded to analyze the crystalline/amorphous nature of CNPs. The SAED patterns show diffused halo rings without spots or solid ring patterns, indicating the amorphous nature of CNPs.[44,45] The diffused halo ring pattern is a common feature in highly disordered amorphous carbon nanomaterials.

The CNPs were characterized by X-ray photoelectron spectroscopy (XPS) and the survey spectra (Fig. S17–S22 and Table S2†) shows peaks for carbon, oxygen and nitrogen. The presence of major peaks at 284.5 eV associated with carbon (83.4%; Table 2) atoms confirmed the presence of carbonaceous materials. However, the presence of a significant amount of oxygen (14.2%) and nitrogen (2.4%) atoms could be attributed to PVPVA and surfactant (Triton X-45) still present in the sample, likely surrounding the CNPs. The oxygen-to-carbon ratio was calculated to be 0.17 for CNPs from the atomic% values measured by XPS survey spectra as shown in Tables 2 and S2.† The ratio varied only slightly with the increase in the reaction temperature and reaction time, meaning that these parameters do not significantly impact the chemical composition of the CNPs.

X-ray induced Auger electron spectroscopy is used to study the ratio of carbon hybridization states sp^2/sp^3 for carbon allotropes and polymers.[46,47] XAES was measured from the C KLL spectra recorded along with XPS survey spectra; the first derivative C KLL spectra are shown in Fig. 2a (S23 and S24†). For comparison, XAES spectra of graphite were also recorded. The D-parameter values were calculated as shown in Table S3.† The D-parameter values are varying with the variation in temperature and reaction time. When compared with the D-parameter values of graphite which has 100% sp^2 carbon, it can be observed that the amount of sp^2 carbon in CNPs is increasing with the increase in reaction temperature and time.

It is well known that the C–C/C=C vibrations produce weaker peaks in IR spectroscopy (Fig. S25 and S26†) and stronger ones in Raman spectroscopy. Thus, characterizing CNPs with Raman spectroscopy provides more information about carbon hybridization states. Raman spectrum is shown in Fig. 2b. As usually observed for CNPs made from the

Table 2 Summary of atomic% values of elements (C, O, N) in CNPs from XPS survey spectra shown in Fig. S22 (ESI)

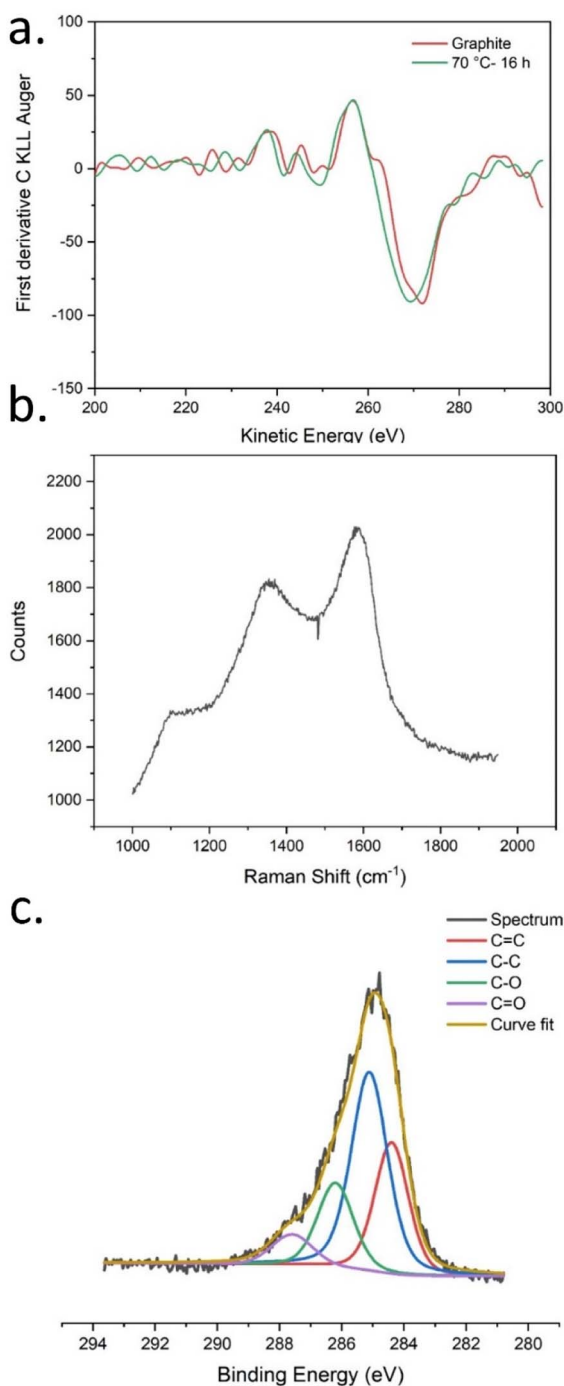| Elements	Atomic (%)
C	83.4
O	14.2
N	2.4
O/C	0.17

Fig. 2 (a) First derivative CKLL XAES spectrum for CNPs and graphite, (b) Raman spectrum, (c) high-resolution XPS C 1s spectra of CNPs synthesized at 70 °C for 16 hours.

values are not absolute values, the ratio of the peak percentage values was compared, and the peaks were grouped as CC peaks (C–C and C=C) and CO peaks (C–O and C=O). Interestingly, the CO/CC peak ratio changed when the reaction parameters were varied as shown in Table S10.† The increase in temperature causes an increase in the relative abundance of C–O/C=O groups with respect to C–C/C=C, which is evident by an increase in their relative peak ratio with the increase in reaction temperature and reaction time.

To study the optical properties of CNPs, UV-visible absorption spectra and photoluminescence spectra were recorded. The UV-visible spectrum (Fig. S32 and S33†) exhibits a very typical absorption pattern for carbon nanomaterials specifically carbon dots,[49-51] with absorption peaks at 251 nm, 276 nm, 284 nm and 327 nm. The CNPs were excited at these wavelengths and the resulting photoluminescence spectra show emission in both the UV and visible regions around 600 nm as shown in Fig. 3a (and S34–S38†). These results suggest that there are luminescent fragments embedded within the CNPs structure that are emissive in the UV region. One way to create an emissive domain is to promote further graphitization of the sp^2 carbon network. This can be achieved by thermal annealing[52] or irradiation.[13] In fact, the polyynes and their partially decomposed products are known to be metastable meaning that they can be chemically transformed into large π-conjugated domains when exposed to heat or light.[37,48] To keep the structural integrity of the CNPs, UV irradiation was preferred.[19,42] Irradiation of the CNPs was performed on CNP dispersion in acetonitrile using a photoreactor
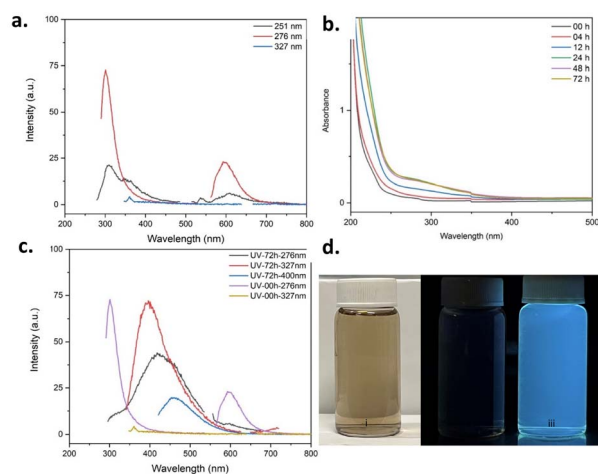

Fig. 3 (a) Photoluminescence spectra recorded in methanol at excitation wavelengths (251 nm, 276 nm, 327 nm) for CNPs synthesized at 70 °C for 16 hours; (c) photoluminescence spectra at excitation wavelengths (276 nm and 327 nm) before (00h) and after (72 h) of UV irradiation for CNPs dispersed in acetonitrile for synthesized at 70 °C for 16 hours. The discontinuity of spectra is due to the removal of second harmonics peaks. (b) UV-vis. absorption spectra recorded in methanol at various time intervals before (00h) and after UV irradiation of CNPs dispersed in acetonitrile for CNPs synthesized at 70 °C for 16 hours; (d) Photographic images of CNPs synthesized at 70 °C for 16 hours, observed (i) in daylight, (ii) under UV lamp, (iii) CNPs after 72 hours of UV-irradiation under a UV-lamp.

decomposition of alkyne-rich molecules,[48] only two broad peaks associated with the D (1350 cm^{-1}) and the G (1590 cm^{-1}) bands are observed, suggesting a disordered graphitic structure.

High-resolution XPS C 1s spectra were recorded and the curve-fitted high-resolution XPS C 1s spectra are shown in Fig. 2c (and S27–S31†). The curve-fitted values for peaks of interest (C–C, C=C, C–O, and C=O) are shown in adjoining tables (Table S4–S9†) for each spectrum. Since the curve fitted

equipped with 16 × 254 nm light bulbs (7.2 W). The CNPs were irradiated for 72 hours, and the absorption and emission were recorded at time intervals (4 h, 12 h, 24 h, 72 h) to study the change in properties. The absorption spectra at various time intervals are shown in Fig. 3b. Interestingly, the absorption intensities changed significantly after 4 h, 12 h, and 24 h of irradiation, but the changes were minimal after 48 h and 72 h. Comparing the absorption spectra before irradiation (00h) and after 72 hours of UV irradiation (Fig. S32, S33 and S39, S40†), it can be observed that the absorption intensities have increased significantly between the 250 nm and 350 nm but no new well-resolved peaks have appeared. The increase in absorption intensities after irradiation indicates that structural changes might have occurred during the irradiation process. Interestingly, the TEM images (Fig. S50 and S51†) after the photochemical treatment show the presence of carbon dots, graphene-like sheets, and aggregates of bigger CNPs along with the spherical CNPs present before UV irradiation indicating changes in the morphology of the CNPs.

The photoluminescence spectra changed significantly upon irradiation as shown in Fig. 3c (and S41–S49†). As expected, a shift in the photoluminescence spectra was observed upon irradiation. The emission shifted from the UV to the visible region, meaning that conjugated fragments with longer effective conjugation length have been formed upon irradiation. Also, the emission peak position is excitation wavelength-dependent, as observed for CNPs prepared using other methods.[44] The CNPs are emitting blue-colored light under UV lamps as shown in Fig. 3d (and Fig. S68–S72†).

XPS survey spectra (Fig. S52–S57†) show an increase in the oxygen content in CNPs after UV irradiation as shown in Tables S11 and S12.† C KLL Auger spectra (Fig. S58 and S59†) of CNPs measured after irradiation show a slight increase in the values of the D-parameter (Table S13†) in comparison to before UV-irradiation (Table S3 and S14†), meaning that light-induced graphitization of CNPs took place. The FT-IR measurements (Fig. S60 and S61†) and high-resolution C 1s spectra (Fig. S62–S67 and Tables S15–S22†) show the increased presence of the oxygen species after UV irradiation. Indeed, we observe an increase in the CO/CC ratios (Tables S21 and S22†) in comparison to before UV-irradiation (Tables S9 and S22†). The increase in the oxygen content (O/C ratio: Table S12†), increased graphitization (Table S14†) and increased presence of oxygen-based functional groups (CO/CC ratio: Table S22†), should be responsible for the change in the emission properties and shift of emission peaks towards the visible region from the UV region after irradiation. Thus, one can argue that the change in the emission properties of the CNPs upon irradiation can be attributed to the formation of additional emissive domains as well as the presence of carbonyl groups as a result of partial photo-oxidation of the NPs.

Conclusions

In conclusion, the dispersion polymerization of acetylene was successful in synthesizing CNPs from acetylene gas and modulating their optical properties. The synthesis of CNPs was achieved by the polymerization of acetylene at low temperature with Glaser-type Pd-catalyzed homocoupling in a dispersion polymerization medium at low temperature. This demonstrates the first use of acetylene gas in a dispersion polymerization reaction for the synthesis of CNPs with controlled morphology. The polymerization method was optimized to synthesize spherical CNPs with narrow size distribution. The UV irradiation of CNP dispersion changed the emission of CNPs from the UV region to the visible region. The presence and transformation of residual alkynes show that residual alkynes could be used to attach functional groups to add new properties to the CNPs.

Author contributions

VKJ: conceptualization, methodology, investigation, formal analysis, data curation, visualization, validation, writing – original draft, writing – review & editing. AMR: funding acquisition, resources methodology, supervision, validation, writing – review & editing. JFM: conceptualization, funding acquisition, resources, methodology, supervision, formal analysis, validation, writing – original draft, writing – review & editing, project administration.

Conflicts of interest

Authors declare that there are no conflicts.

Acknowledgements

References

1 X. Xu, R. Ray, Y. Gu, H. J. Ploehn, L. Gearheart, K. Raker, et al., Electrophoretic Analysis and Purification of Fluorescent Single-Walled Carbon Nanotube Fragments, J. Am. Chem. Soc., 2004, 126(40), 12736–12737.

2 D. Pan, J. Zhang, Z. Li, C. Wu, X. Yan and M. Wu, Observation of pH-, solvent-, spin-, and excitation-dependent blue photoluminescence from carbon nanoparticles, Chem. Commun., 2010, 46(21), 3681–3683.

3 L. Xiao, Y. Cao, W. A. Henderson, M. L. Sushko, Y. Shao, J. Xiao, et al., Hard carbon nanoparticles as high-capacity, high-stability anodic materials for Na-ion batteries, Nano Energy, 2016, 19, 279–288.

4 W. K. Oh, H. Yoon and J. Jang, Size control of magnetic carbon nanoparticles for drug delivery, Biomaterials, 2010, 31(6), 1342–1348.

5 Y. Fang, S. Guo, D. Li, C. Zhu, W. Ren, S. Dong, *et al.*, Easy Synthesis and Imaging Applications of Cross-Linked Green Fluorescent Hollow Carbon Nanoparticles, *ACS Nano*, 2012, **6**(1), 400–409.

6 X. Wang, K. Qu, B. Xu, J. Ren and X. Qu, Multicolor luminescent carbon nanoparticles: Synthesis, supramolecular assembly with porphyrin, intrinsic peroxidase-like catalytic activity and applications, *Nano Res.*, 2011, **4**(9), 908–920.

7 I. V. Gofman, I. V. Abalov, V. G. Tiranov and V. E. Yudin, Effect of carbon nanoparticles of different shapes on mechanical properties of aromatic polyimide-based composite films, *Polym. Sci., Ser. A*, 2013, **55**(5), 313–319.

8 H. Y. Nezhad and V. K. Thakur, Effect of Morphological Changes due to Increasing Carbon Nanoparticles Content on the Quasi-Static Mechanical Response of Epoxy Resin, *Polymers*, 2018, **10**(10), 1106.

9 B. Schulte, S. Schrettl and H. Frauenrath, Synthesis and Use of Reactive Molecular Precursors for the Preparation of Carbon Nanomaterials, *Phys. Sci. Rev.*, 2017, **2**(2), 20160100.

10 T. N. Hoheisel, S. Schrettl, R. Szilluweit and H. Frauenrath, Nanostructured Carbonaceous Materials from Molecular Precursors, *Angew. Chem., Int. Ed.*, 2010, **49**(37), 6496–6515.

11 F. Cataldo, *Polyynes: Synthesis, Properties, and Applications*, Taylor & Francis, Boca Raton, FL, 2006, available from: http://www.crcnetbase.com/isbn/9781574445121.

12 E. T. Chernick and R. R. Tykwinski, Carbon-rich nanostructures: the conversion of acetylenes into materials, *J. Phys. Org. Chem.*, 2013, **26**(9), 742–749.

13 S. Rondeau-Gagné and J.-F. Morin, Preparation of carbon nanomaterials from molecular precursors, *Chem. Soc. Rev.*, 2014, **43**(1), 85–98.

14 F. Banhart, Formation and transformation of carbon nanoparticles under electron irradiation, *Philos. Trans. R. Soc., A*, 2004, **362**(1823), 2205–2222.

15 J. Hlavatý, L. Kavan, N. Kasahara and A. Oya, Polymerisation of 1-iodohexa-1,3,5-triyne and hexa-1,3,5-triyne: a new synthesis of carbon nanotubes at low temperatures, *Chem. Commun.*, 2000, (9), 737–738.

16 H. Xie, Y. Zhao, Y. Tian, X. Wang and M. Yan, Tailored synthesis from rhombic dodecahedron to spherical ordered mesoporous carbon nanoparticles via one-step strategy, *Carbon*, 2019, **152**, 295–304.

17 Y.-J. Zhan and S.-H. Yu, Direct Synthesis of Carbon-Rich Composite Sub-microtubes by Combination of a Solvothermal Route and a Succeeding Self-Assembly Process, *J. Phys. Chem. C*, 2008, **112**(11), 4024–4028.

18 Y.-S. Sun, W.-H. Huang, C.-F. Lin and S.-L. Cheng, Tailoring Carbon Nanostructure with Diverse and Tunable Morphology by the Pyrolysis of Self-Assembled Lamellar Nanodomains of a Block Copolymer, *Langmuir*, 2017, **33**(8), 2003–2010.

19 A. Picard-Lafond and J.-F. Morin, Low-Temperature Synthesis of Carbon-Rich Nanoparticles with a Clickable Surface for Functionalization, *Langmuir*, 2017, **33**(22), 5385–5392.

20 M. Escobar, M. S. Moreno, R. J. Candal, M. C. Marchi, A. Caso, P. I. Polosecki, *et al.*, Synthesis of carbon nanotubes by CVD: Effect of acetylene pressure on nanotubes characteristics, *Appl. Surf. Sci.*, 2007, **254**(1), 251–256.

21 R. Atchudan, S. Perumal, T. N. Jebakumar Immanuel Edison and Y. R. Lee, Highly graphitic carbon nanosheets synthesized over tailored mesoporous molecular sieves using acetylene by chemical vapor deposition method, *RSC Adv.*, 2015, **5**(113), 93364–93373.

22 M. Choi, I. S. Altman, Y. J. Kim, P. V. Pikhitsa, S. Lee, G. S. Park, *et al.*, Formation of Shell-Shaped Carbon Nanoparticles Above a Critical Laser Power in Irradiated Acetylene, *Adv. Mater.*, 2004, **16**(19), 1721–1725.

23 T.-C. Liu and Y.-Y. Li, Synthesis of carbon nanocapsules and carbon nanotubes by an acetylene flame method, *Carbon*, 2006, **44**(10), 2045–2050.

24 S. Delpeux, K. Szostak, E. Frackowiak, S. Bonnamy and F. Béguin, High Yield of Pure Multiwalled Carbon Nanotubes from the Catalytic Decomposition of Acetylene on in Situ Formed Cobalt Nanoparticles, *J. Nanosci. Nanotechnol.*, 2002, **2**(5), 481–484.

25 M. H. Khedr, K. S. Abdel Halim and N. K. Soliman, Effect of temperature on the kinetics of acetylene decomposition over reduced iron oxide catalyst for the production of carbon nanotubes, *Appl. Surf. Sci.*, 2008, **255**(5), 2375–2381.

26 Y. T. Lee, N. S. Kim, J. Park, J. B. Han, Y. S. Choi, H. Ryu, *et al.*, Temperature-dependent growth of carbon nanotubes by pyrolysis of ferrocene and acetylene in the range between 700 and 1000 °C, *Chem. Phys. Lett.*, 2003, **372**(5), 853–859.

27 M. Hundt, P. Sadler, I. Levchenko, M. Wolter, H. Kersten and K. Ostrikov, Real-time monitoring of nucleation-growth cycle of carbon nanoparticles in acetylene plasmas, *J. Appl. Phys.*, 2011, **109**(12), 123305.

28 R. Atchudan, S. Perumal, T. N. J. I. Edison, A. Pandurangan and Y. R. Lee, Synthesis and characterization of graphenated carbon nanotubes on IONPs using acetylene by chemical vapor deposition method, *Phys. E*, 2015, **74**, 355–362.

29 Y. V. Fedoseeva, K. M. Popov, G. A. Pozdnyakov, V. N. Yakovlev, B. V. Sen'kovskiy, L. G. Bulusheva, *et al.*, Structure of carbon nanoparticles synthesized by adiabatic compression of acetylene and their application in supercapacitors, *J. Struct. Chem.*, 2017, **58**(6), 1196–1204.

30 Y. Qin, X. Jiang and Z. Cui, Low-Temperature Synthesis of Amorphous Carbon Nanocoils via Acetylene Coupling on Copper Nanocrystal Surfaces at 468 K: A Reaction Mechanism Analysis, *J. Phys. Chem. B*, 2005, **109**(46), 21749–21754.

31 Y. V. Surovikin, A. G. Shaitanov, A. V. Lavrenov and D. A. Shlyapin, New approaches to the production of acetylene carbon black, *AIP Conf. Proc.*, 2020, **2301**(1), 040015.

32 A. S. Hay, Oxidative polymerization of diethynyl compounds, *J. Polym. Sci., Part A-1: Polym. Chem.*, 1969, **7**(7), 1625–1634.

33 H. Matsuda, H. Nakanishi and M. Kato, Conducting Polyyne and Poly(rnetal-yne) from Butadiyne, *J. Polym. Sci., Polym. Lett. Ed.*, 1984, **22**, 107–111.

34 K. Ohmura, M. Kijima and H. Shirakawa, Synthesis of conducting polymers with conjugated carbon-carbon triple bonds by electrochemical condensation of acetylene derivatives catalyzed by copper complex, *Synth. Met.*, 1997, **84**, 417–418.

35 M. Kijima, Y. Sakai and Shnakawa II, Electrochemical synthesis of carbyne catalyzed by nickel complex, *Synth. Met.*, 1995, **71**, 1837–1840.

36 Y. P. Kudryavtsev, R. B. Heimann and S. E. Evsyukov, Review Carbynes: advances in the field of linear carbon chain compounds, *J. Mater. Sci.*, 1996, **31**, 5557–5571.

37 I. Levesque, J. R. Néabo, S. Rondeau-Gagné, C. Vigier-Carrière, M. Daigle and J.-F. Morin, Layered graphitic materials from a molecular precursor, *Chem. Sci.*, 2014, **5**(2), 831–836.

38 A. J. C. Kuehne, M. C. Gather and J. Sprakel, Monodisperse conjugated polymer particles by Suzuki–Miyaura dispersion polymerization, *Nat. Commun.*, 2012, **3**(1), 1088.

39 N. Anwar, T. Willms, B. Grimme and A. J. C. Kuehne, Light-Switchable and Monodisperse Conjugated Polymer Particles, *ACS Macro Lett.*, 2013, **2**(9), 766–769.

40 J. B. ten Hove, J. Appel, J. M. van den Broek, A. J. C. Kuehne and J. Sprakel, Conjugated Polymer Shells on Colloidal Templates by Seeded Suzuki–Miyaura Dispersion Polymerization, *Small*, 2014, **10**(5), 957–963.

41 R. R. Rosencrantz, K. Rahimi and A. J. C. Kuehne, Morphology Control in Poly(9,9-di-n-octyl-2,7-fluorene) Spherulite Particles Prepared via Dispersion Polymerization, *J. Phys. Chem. B*, 2014, **118**(23), 6324–6328.

42 A. Picard-Lafond, M. Daigle and J.-F. Morin, Tetraphenylethene–diyne hybrid nanoparticles from Glaser-type dispersion polymerization, *RSC Adv.*, 2017, **7**(57), 36132–36137.

43 N. Anwar, A. Rix, W. Lederle and A. J. C. Kuehne, RGD-decorated conjugated polymer particles as fluorescent biomedical probes prepared by Sonogashira dispersion polymerization, *Chem. Commun.*, 2015, **51**(45), 9358–9361.

44 C. Wu, C. Wei, X. Jin, R. Akhtar and W. Zhang, Carbon spheres as lubricant additives for improving tribological performance of polyetheretherketone, *J. Mater. Sci.*, 2018, **54**(6), 5127–5135.

45 A. B. Siddique, V. Pratap Singh, S. Chatterjee, A. Kumar Pramanik and M. Ray, Facile synthesis and versatile applications of amorphous carbon dot, *Mater. Today: Proc.*, 2018, **5**(3), 10077–10083.

46 B. Lesiak, L. Kövér, J. Tóth, J. Zemek, P. Jiricek, A. Kromka, *et al.*, C sp2/sp3 hybridisations in carbon nanomaterials – XPS and (X)AES study, *Appl. Surf. Sci.*, 2018, **452**, 223–231.

47 S. Y. Lee, J. Lyu, S. Kang, S. J. Lu and C. W. Bielawski, Ascertaining the Carbon Hybridization States of Synthetic Polymers with X-ray Induced Auger Electron Spectroscopy, *J. Phys. Chem. C*, 2018, **122**(22), 11855–11861.

48 J. R. Néabo, C. Vigier-Carrière, S. Rondeau-Gagné and J.-F. Morin, Room-temperature synthesis of soluble, fluorescent carbon nanoparticles from organogel precursors, *Chem. Commun.*, 2012, **48**(81), 10144–10146.

49 W.-S. Zou, W.-L. Kong, Q.-C. Zhao, J. Zhang, X. Zhao, D. Zhao, *et al.*, A composite consisting of bromine-doped carbon dots and ferric ions as a fluorescent probe for determination and intracellular imaging of phosphate, *Microchim. Acta*, 2019, **186**(8), 576.

50 P. Paoprasert, H. Moonmuang, P. Supchocksoonthorn, N. Thongsai and S. Kladsomboon, Black sesame-derived carbon dots for metal ion and amine vapour sensing, *IOP Conf. Ser.: Mater. Sci. Eng.*, 2018, **378**, 012003.

51 M. He, J. Zhang, H. Wang, Y. Kong, Y. Xiao and W. Xu, Material and Optical Properties of Fluorescent Carbon Quantum Dots Fabricated from Lemon Juice via Hydrothermal Reaction, *Nanoscale Res. Lett.*, 2018, **13**(1), 175.

52 X. Miao, D. Qu, D. Yang, B. Nie, Y. Zhao, H. Fan, *et al.*, Synthesis of Carbon Dots with Multiple Color Emission by Controlled Graphitization and Surface Functionalization, *Adv. Mater.*, 2018, **30**(1), 1704740.